

# Optical generation of pure spin currents at the indirect gap of bulk Si

F. Bottegoni,<sup>a)</sup> C. Zucchetti, F. Ciccacci, M. Finazzi, and G. Isella

LNESS-Dipartimento di Fisica, Politecnico di Milano, Piazza Leonardo da Vinci 32, 20133 Milano, Italy

(Received 28 October 2016; accepted 11 January 2017; published online 24 January 2017)

We report on the optical generation of a pure spin current at the indirect gap of bulk Si at room temperature in the photon energy range comprised between 1.2 and 1.8 eV. Spin-polarized electrons are promoted to the  $\Delta$ -valleys of the Si Brillouin zone by circularly polarized light. The photo-generated spin current is then detected by exploiting a Schottky Pt/Si(001) junction: spin-polarized electrons diffuse toward the Pt/Si interface and enter the Pt layer where the spin current is converted into a transverse electromotive field through the inverse spin-Hall effect (ISHE). The photon energy dependence of the ISHE signal is interpreted in the frame of a one-dimensional spin drift-diffusion model, which allows estimating the electron spin lifetime to be  $\tau_s = 15 \pm 5$  ns.

Published by AIP Publishing. [<http://dx.doi.org/10.1063/1.4974820>]

One of the most important goals of spintronics is to combine electronic and spin degrees of freedom of carriers on the Si platform to handle classical or quantum information. In this frame, optical spin orientation, i.e., the possibility of optically exciting spin-polarized electrons by means of circularly polarized light,<sup>1</sup> is a powerful tool to explore spin transport and dynamics in semiconductors.<sup>2</sup> The optical injection of spin-oriented electrons was first achieved by Lampel in Si at low temperature.<sup>3</sup> However, after this pioneering study, the low spin-orbit interaction and the long carrier lifetime in bulk Si<sup>4,5</sup> have prevented further optical investigations of spin generation and transport in Si, and optical orientation studies have been almost completely focused on III–V semiconductors,<sup>2,6–9</sup> with a few reports on Ge<sup>10–12</sup> and, more recently, on SiGe heterostructures.<sup>13,14</sup>

In optical spin orientation, dipole selection rules for optical transitions with circularly polarized light allow for the generation of a spin-oriented electron population in the conduction band of the semiconductor. Defining  $n_{\uparrow(\downarrow)}$ , the up-(down-) spin densities referred to the quantization axis given by the direction of light propagation in the material, the spin polarization can be written as  $P = (n_{\uparrow} - n_{\downarrow}) / (n_{\uparrow} + n_{\downarrow})$ . The spin-orbit interaction plays a key role in the determination of  $P$ : both in GaAs and Ge, the energy separation between heavy hole (HH)-light hole (LH) and split-off (SO) states in the valence band at  $\Gamma$  is  $\Delta E_{SO} \approx 300$  meV so that the incident photon energy can be easily tuned to promote in the conduction band only electrons coming from HH and LH states. As a consequence, in bulk GaAs- and Ge-based semiconductors, spin polarization values approaching  $P \approx 50\%$  can be achieved.

In bulk Si, the scenario is radically different: the direct bandgap at  $\Gamma$  lies in the ultraviolet range ( $E_{dg} = 4.2$  eV at room temperature), and the energy difference between HH-LH and SO states is only  $\Delta E_{SO} \approx 40$  meV, whereas the fundamental gap is indirect ( $E_{ig} = 1.12$  eV at room temperature). Nevertheless, theoretical calculations indicate that phonon-assisted optical transitions at the indirect gap of Si can generate a spin-oriented electron population with  $P \approx 5\%$ ,<sup>15,16</sup> and

indeed experimental evidence of optical spin orientation in Si has been obtained but only at cryogenic temperatures<sup>3</sup> and with the use of fairly large magnetic fields.<sup>17</sup>

In recent years, the exploitation of electrical spin-injection schemes, at both low<sup>18–24</sup> and room temperatures,<sup>25–28</sup> and the prediction of large intrinsic electron spin lifetimes<sup>29–34</sup> have renewed the interest of the spintronic community for bulk Si and Si-based heterostructures.<sup>31</sup> In this framework, the exploitation of optical orientation in Si would add a relevant building block for the design of spintronic devices on a single material platform.

In this paper, we report on the optical generation of a pure spin current at the indirect gap of bulk Si(001) at room temperature. To this purpose, we have combined optical orientation with an electrical detection scheme based on the inverse spin-Hall effect (ISHE),<sup>35</sup> which takes place within a Pt layer forming a Schottky junction with the investigated sample. Such a photo-induced ISHE approach has been already used to detect optically excited spins at the direct gap of GaAs,<sup>36–38</sup> InP,<sup>39</sup> and Ge.<sup>40–42</sup>

The photo-induced ISHE signal has been measured in a Pt/n-doped Si junction: the spin-oriented electrons, generated at the  $\Delta$ -valleys of bulk Si, diffuse toward the Pt/Si interface and yield an electromotive force at the edges of the thin Pt layer through spin-dependent scattering with Pt nuclei. Pt has been chosen as a spin detector due to its large spin-Hall angle.<sup>35</sup> We have also investigated the photon energy dependence of the ISHE signal in the range between  $1.2 < h\nu < 1.8$  eV, and we have interpreted the experimental results by means of a drift-diffusion model,<sup>38</sup> which fairly reproduces the main spectral features and allows for an estimation of the electron spin lifetime at the  $\Delta$  minima giving  $\tau_s = 15 \pm 5$  ns.

The investigated device and the experimental geometry are sketched in Fig. 1(a): a  $l_x \times l_y = 5 \times 5$  mm<sup>2</sup>-wide and 4 nm-thick Pt layer is deposited by e-beam evaporation on top of a 500  $\mu$ m-thick phosphorous-doped Si(001) substrate ( $\rho_{Si} \approx 5 \Omega \cdot \text{cm}$ ; doping concentration,  $N_p \approx 8.95 \times 10^{14} \text{ cm}^{-3}$ ). Two 200 nm-thick Au/Ti contacts are then evaporated at the edges of the Pt layer along the  $y$  axis. The height of the Schottky barrier  $E_B = 0.83$  eV has been measured by

<sup>a)</sup>Electronic mail: federico.bottegoni@polimi.it

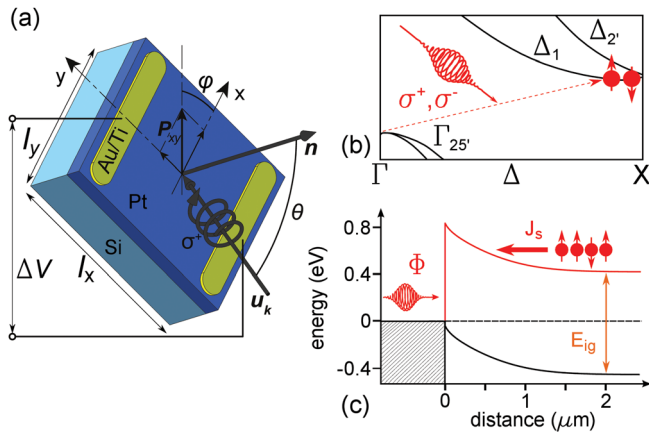


FIG. 1. (a) Scheme of the Pt/Si sample and of the experimental geometry:  $\theta$  is the angle between the direction of the incident light  $\mathbf{u}_k$  and the normal  $\mathbf{n}$  to the sample surface, whereas  $\varphi$  is the angle between the projection of  $\mathbf{u}_k$  in the sample plane and the  $x$  axis. (b) Sketch of the  $\Gamma \rightarrow \Delta$  indirect transitions involved in the optical orientation process. The symmetry of the electronic states according to the notation in Ref. 43 is reported. (c) Pt/Si Schottky junction and band alignment at the Pt/Si interface under illumination with a photon flux  $\Phi$  and open-circuit conditions.

fabricating Pt/Si metal-semiconductor-metal structures and applying the I–V curve analysis reported in Ref. 44.

ISHE measurements have been performed in air at room temperature: spin-polarized electrons are excited by a focused beam (spot size  $d \approx 10 \mu\text{m}$ ) from a Ti:sapphire tunable laser, which provides photons in the 1.2–1.8 eV energy range. The circular polarization of the light is modulated by a photoelastic modulator (PEM) at 50 kHz, and the voltage difference  $\Delta V$  between the two Au/Ti electrodes, separated by about 4 mm, is detected by a lock-in amplifier under open-circuit conditions. The wave-vector of the light inside the semiconductor, which sets the direction of the spin-polarization vector  $\mathbf{P}$ , can be continuously varied by changing the polar angle  $\theta$  and the azimuthal angle  $\varphi$ , defined in Fig. 1(a).

Literature reports indicate that in Si, the hole spin lifetime lies in the hundreds of ps range.<sup>25,26,45</sup> Since the electron spin lifetime exceeds by orders of magnitude this temporal range,<sup>29–34</sup> as also demonstrated in the present paper (see below), the spin signal can be assumed to be mostly related to photo-generated electrons (see Fig. 1(b)). Moreover, even at the lowest excitation energy used in our experiments ( $h\nu = 1.2 \text{ eV}$ ), HH, LH, and SO are all optically excited, thus giving a negligible initial hole spin polarization. This means that, while no charge current is injected or extracted into the semiconductor during our experiments, the two electron spin populations are unbalanced, thus yielding a pure spin current.<sup>40,46</sup> Photo-generated electrons then diffuse towards the Pt/Si interface, crossing a depletion region of  $w_{\text{dep}} = 1.1 \mu\text{m}$ -width in correspondence to the Schottky barrier (see Fig. 1(c)). When the sample is illuminated under open-circuit conditions, the photon flux  $\Phi$  lowers the height of the Schottky barrier (see Fig. 1(c)). Then, electrons are injected into the Pt layer via thermionic emission, carrying a spin current density  $\mathbf{J}_s$ , which is converted into an effective electromotive field  $\mathbf{E}_{\text{ISHE}}$ , yielding a voltage difference  $\Delta V \propto E_{\text{ISHE}}$  between the two Au/Ti electrodes,<sup>36,42</sup> where  $\mathbf{E}_{\text{ISHE}} = D_{\text{ISHE}} \cdot (\mathbf{J}_s \times \mathbf{P})$ ,  $D_{\text{ISHE}}$  being the efficiency of the ISHE process.<sup>35</sup>

The spin-related nature of the detected signal has been verified by varying the projection of the spin polarization vector  $\mathbf{P}$  along the  $x$  axis. The dependence of the voltage difference  $\Delta V$  as a function of the angle  $\theta$  for  $\varphi = 0$ , an incident photon energy of  $h\nu = 1.37 \text{ eV}$ , and an incident power of  $W = 1 \text{ mW}$  is shown in Fig. 2(a) (black squares). The error bars take into account the  $\Delta V$  variations between different datasets, originating from possible optical misalignments.

A multilayer optical analysis on the Pt/Si junction indicates that  $\Delta V(\theta, \varphi) \propto t_{sp} \cos \delta \cos \varphi \tan \theta$ ,<sup>47</sup> where  $t_{s(p)}$  is the transmission coefficient of the  $s(p)$ -polarized light and  $\delta$  is the angle between the light propagation wavevector inside Si and the normal to the sample surface. From the transmission coefficients at  $h\nu = 1.37 \text{ eV}$  listed in Refs. 48 and 49 for Pt and Si, respectively, one can explicitly calculate the dependence of  $\Delta V$  on  $\theta$  (red dashed line in Fig. 2(a)) and  $\varphi$  (red dashed line in Fig. 2(b)) and compare it to the experimental data in Fig. 2. The good agreement that we find between the calculation and the experiment confirms the spin-related origin of the measured signal.

As a further independent confirmation of the spin-related nature of the measured signal, we have performed measurements on a 4 nm-thick Cu/Si sample under the same experimental conditions. The substitution of a high-Z material (Pt) with a low-Z one (Cu) should lead to a strong reduction in the spin-orbit scattering and a vanishing ISHE signal. The corresponding  $\theta$ -dependence of the ISHE signal for this case is shown as red dots in Fig. 2(a): indeed, a negligible  $\Delta V$  has been detected for all the incident angles.

The  $\Delta V$  dependence on the degree of circular polarization of the incident light ( $P_{\text{circ}}$ ) is reported in Fig. 3(a) for  $h\nu = 1.37 \text{ eV}$  and  $W = 1 \text{ mW}$ : in this case, the measurements have been performed by varying the phase retardation  $\Delta\zeta$  of the PEM. Indeed, the temporal dependence of  $P_{\text{circ}}$  can be expressed as  $P_{\text{circ}} = -\sin[\Delta\zeta \cos(\omega t)]$ : then the Fourier series expansion, truncated to the first harmonic, yields  $P_{\text{circ}} \approx -2J_1(\Delta\zeta) \cos(\omega t)$ , where  $J_1(\Delta\zeta)$  is the Bessel function of the first order. The experimental data shown in Fig. 3(a) reproduce the expected behaviour of  $\Delta V$  as a function of  $P_{\text{circ}}$ .

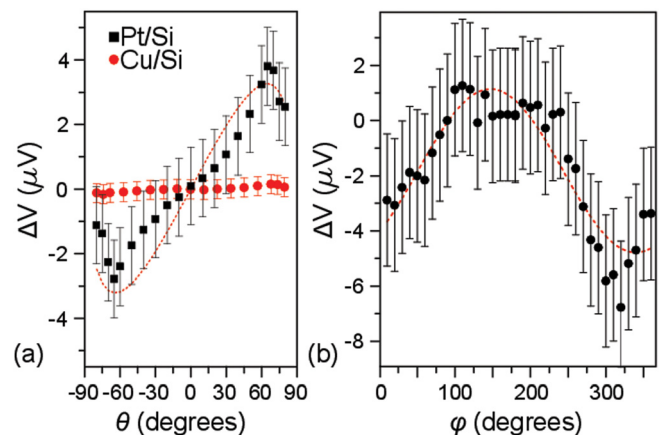


FIG. 2. (a) ISHE signal dependence as a function of the angle  $\theta$  for the Pt/Si (black squares) and Cu/Si (red dots) junctions for fixed  $\varphi = 0$ . (b) ISHE signal dependence as a function of the angle  $\varphi$  for a fixed  $\theta = 65^\circ$ . The measurements have been performed with a photon energy of  $h\nu = 1.37 \text{ eV}$  and an incident power of  $W = 1 \text{ mW}$ . The red dashed line corresponds to the  $\cos \delta \tan \theta$ -dependence (a) and  $\cos \varphi$ -dependence (b), obtained from a multilayer optical analysis of the Pt/Si junction.

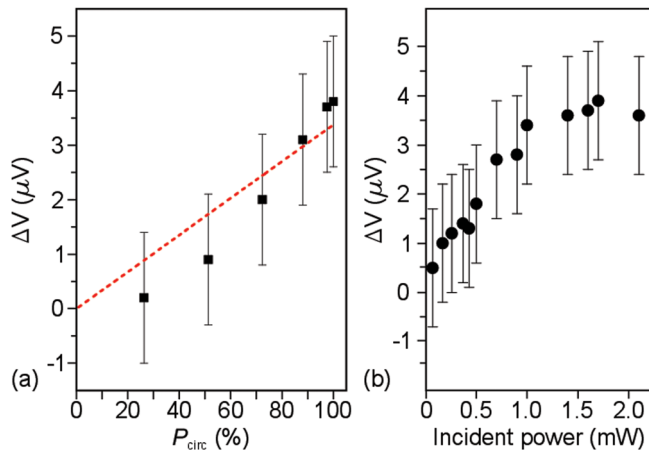


FIG. 3. (a) ISHE signal dependence as a function of the degree of circular polarization of the light ( $P_{\text{circ}}$ ) for an incident photon energy of  $h\nu = 1.37$  eV and an incident power  $W = 1$  mW. The red dashed line is a linear fit to  $\Delta V$ . (b)  $\Delta V$  dependence as a function of  $W$  for an incident photon energy of  $h\nu = 1.37$  eV.

The power dependence of the ISHE signal (see Fig. 3(b)) mirrors the behaviour of the photovoltage across a metal/semiconductor Schottky contact.<sup>42</sup> It monotonically increases for incident powers below  $\approx 1$  mW and saturates at higher illumination intensities. Therefore, we can infer that in these experimental conditions, the limiting photovoltage  $V_{\text{oc}}$  is reached at approximately 1 mW. In the ideal case of negligible bulk and surface recombination,  $V_{\text{oc}}$  should approach the Schottky barrier height  $E_B$ . However, in real systems,  $V_{\text{oc}}$  can be substantially lower than  $E_B$ ; therefore, a proper estimation of the built-in potential reduction cannot be made for the sample analyzed in the present work.

The maximum absolute value of the ISHE signal for an incident power of  $W = 1$  mW, corresponding to  $\Delta V = 3.5 \pm 1.2 \mu V$ , is obtained for  $\theta = \pm 65^\circ$ , and it is comparable with the one detected in Pt/Ge junctions under the same experimental conditions.<sup>42</sup> According to the theoretical calculations reported

in Ref. 16, phonon-assisted optical transitions for  $h\nu = 1.37$  eV should generate a net electron spin polarization  $P \approx 0.7\%$  (see below, Fig. 4(a)).

In Fig. 4(b), we report the photon energy dependence of the ISHE signal (full dots) in the 1.2–1.8 eV energy range, normalized to the incident photon flux  $\Phi$ .  $\Delta V$  increases with  $h\nu$  up to  $h\nu \approx 1.4$  eV, where we detect a broad maximum, and then it reaches a plateau. The spectral evolution of the experimental data can be interpreted in the frame of a one-dimensional spin drift-diffusion model,<sup>2,38</sup> neglecting as a first approximation the spin and charge diffusion in the plane of the sample. The spin density  $s$  and the spin current density  $J_s$  inside the semiconductor are defined as  $s = n_\uparrow - n_\downarrow$  and  $J_s = q(J_\uparrow - J_\downarrow)$ , where  $J_{\uparrow(\downarrow)}$  is the spin-up(down) current density related to the photo-generated spin-polarized electrons. The spatial distribution of  $s$  and  $J_s$  can be described through the equations

$$\frac{1}{q} J_s(x) = -D_n \frac{\partial s(x)}{\partial x} - \mu_n s(x) E(x), \quad (1a)$$

$$\frac{1}{q} \frac{\partial J_s(x)}{\partial x} = -\frac{s(x)}{\tau_s} - w(x)s(x)p(x) + P\Phi\alpha e^{-\alpha x}. \quad (1b)$$

The electric field  $E(x)$ , hole density  $p(x)$ , and the intrinsic generation-recombination rate  $w(x)$  are obtained by numerically solving the coupled Poisson drift-diffusion equations<sup>50</sup> for electrons and holes photo-generated inside the semiconductor by the photon flux  $\Phi$ . The electron mobility  $\mu_n = 1380 \text{ cm}^2 \text{ Vs}^{-1}$ , diffusion coefficient  $D_n = \mu_n k_B T$  ( $k_B$  and  $T$  being the Boltzmann constant and the temperature, respectively), and Shockley-Read-Hall recombination parameters [used for the calculation of  $w(x)$ ] are those typically employed for micro-electronic device simulations.<sup>51</sup> The absorption coefficient  $\alpha$  and initial degree of electron spin polarization  $P$  are extracted from Refs. 49 and 16, respectively, and reported in the inset of Fig. 4(a).

At room temperature and relatively low doping densities, electron-phonon interactions determine the momentum

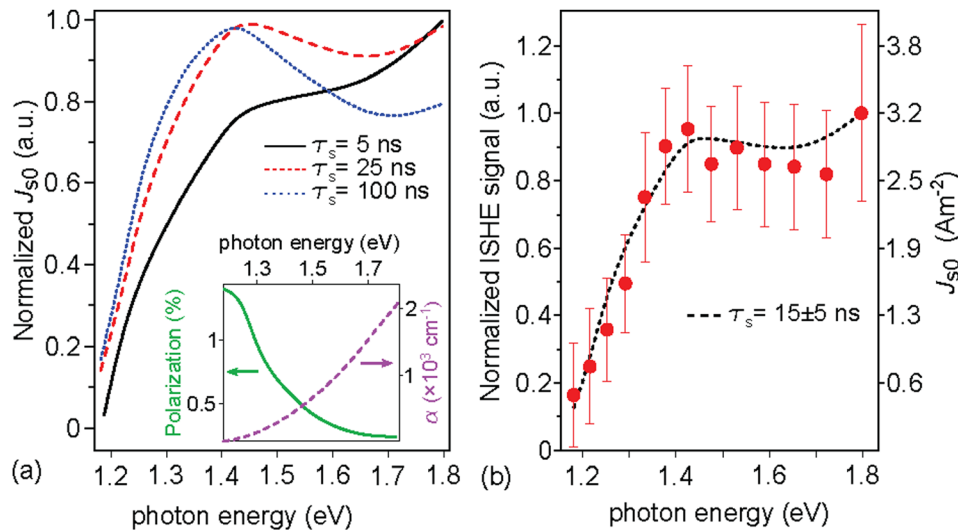


FIG. 4. (a) Normalized  $h\nu$ -dependence of  $J_{s0}$  from Eq. (1) for electron spin lifetimes  $\tau_s = 5$  (continuous black line), 25 (red dashed line), and 100 ns (blue dotted line). Inset: absorption coefficient  $\alpha$  and initial degree of electron spin polarization  $P$  from Refs. 49 and 16, respectively, as a function of the incident photon energy. (b) ISHE signal, as a function of the incident photon energy, normalized with respect to the incident photon flux  $\Phi$  (red dots). The black dashed curve identifies the fitting function calculated with  $\Phi = 10^{18} \text{ cm}^{-2}$ , obtained by solving Eq. (1) for the best fit parameter  $\tau_s = 15 \pm 5$  ns, which corresponds to the spin lifetime of electrons thermalized at the bottom of the Si conduction band.



relaxation time  $\tau_p$  for  $\Delta$ -valley electrons.<sup>52</sup> In this case, the electron spin lifetime  $\tau_s$  is dominated by the Yafet-Elliott mechanism and can therefore be expressed as  $\tau_s(E_k)^{-1} \propto [\Delta_{so}/(E_g + \Delta_{so})]^2 (E_k/E_g)^2 \tau_p(E_k)^{-1}$ , where  $E_k$  is the electron kinetic energy,  $E_g$  the energy gap, and  $\Delta_{so}$  the spin-orbit splitting.<sup>2</sup> Therefore, for Si,  $\tau_s$  is expected to be approximately three orders of magnitude longer than  $\tau_p$ . In Si,  $\tau_p \approx 30$  fs,<sup>53</sup> which implies  $\tau_s$  values in the nanosecond range. On the other hand, the energy relaxation time  $\tau_{en}$ , i.e., the average time required for hot electrons to thermalize at the bottom of the conduction band, is  $\tau_{en} \approx 260$  fs.<sup>53</sup> Since  $\tau_{en} \ll \tau_s$ , most of the scattering events leading to spin relaxation will take place after electron thermalization, and it is therefore a good approximation to consider  $\tau_s$  independent of  $E_k$ , i.e., of the photon energy. By solving Eq. (1), we can calculate the spin current density  $J_{s0}$  injected from the semiconductor into the Pt layer as a function of the incident photon energy taking  $\tau_s$  as a free fitting parameter.

Fig. 4(a) shows the normalized  $h\nu$ -dependence of  $J_{s0}$  for  $\tau_s = 5, 25$ , and  $100$  ns (black continuous, red dashed, and blue dotted lines, respectively, in Fig. 4(a)). The spectral evolution of  $J_{s0}$  can be interpreted in terms of the interplay between the photon energy dependence of  $\alpha$  and  $P$ , reported in the inset of Fig. 4(a). For  $h\nu = 1.18$  eV, electrons are mostly generated with a spin polarization  $P \approx 1.4\%$  in a region relatively far from the Pt/Si interface due to the low value of the absorption coefficient  $\alpha$ . As a consequence, the spin current at the Pt/semiconductor interface is relatively small. For  $h\nu \rightarrow 1.8$  eV, an increasing spin density is generated close to the Pt layer, and despite the lower initial polarization,  $J_{s0}$  increases. It is interesting to note that the overall photon-energy dependence of  $J_{s0}$  is relatively sensitive to the value of  $\tau_s$ , qualitatively reproducing the experimental data of Fig. 4(b) in which the fitting is performed by considering  $\tau_s$  and the proportionality constant between  $J_{s0}$  and the ISHE signal as free parameters.

The best fit of the experimental photon energy dependence of Fig. 4(b) is thus obtained for  $\tau_s = 15 \pm 5$  ns (black dashed line) with an incident photon flux  $\Phi = 10^{18} \text{ cm}^{-2}$ , which is in good agreement with theoretical calculations reported in the literature.<sup>29,52,54</sup> The simple drift-diffusion model of Eq. (1) nicely reproduces the experimental data, unraveling the fundamental issues of spin diffusion at the  $\Delta$  minima of Si: the spin current density  $J_{s0}$  at the Pt/Si interface is dictated by the trade-off between the absorption coefficient  $\alpha$ , which is very small in bulk Si especially close to the indirect bandgap, and the spin polarization  $P$ . Moreover, our experimental estimation of  $\tau_s$  corresponds to a spin diffusion length  $L_s = \sqrt{D_n \tau_s} = 7 \pm 2 \mu\text{m}$ . Such a value exceeds the standard size of common electronic building blocks and suggests that bulk Si can play a central role in the design of novel spintronic devices.

It is interesting to remark that the ISHE signal in Pt/Ge and Pt/Si junctions is of the same order of magnitude for similar Pt thicknesses. In bulk Ge, the maximum ISHE signal is obtained for a photon energy of  $h\nu = 0.8$  eV: in this case, the optical orientation process generates an initial spin polarization  $P \approx 50\%$  at the direct Ge bandgap.<sup>11,41,55</sup> This value is then partially lowered by the ultrafast  $\Gamma - L$  scattering, which electrons undergo in the Ge conduction band.<sup>13</sup> In Si,

the spin current generation and diffusion both take place at the  $\Delta$ -valleys: the maximum  $\Delta V$  is detected for  $h\nu \approx 1.4$  eV, but the initial spin polarization is much smaller. However, the larger spin lifetime ( $\tau_s \approx 1$  ns and  $\approx 15$  ns in bulk Ge and Si, respectively, at room temperature and for lightly doped samples<sup>40,56–58</sup>) allows for an ISHE signal, which is comparable to the one detected in bulk Ge.

In conclusion, we have experimentally demonstrated optical spin orientation at the indirect gap of Si at room temperature. The inverse spin-Hall effect in a Pt/Si junction has been used to detect spin current density generated for photon energies comprised between 1.2 and 1.8 eV. The photon energy dependence of the ISHE signal can be interpreted by means of a spin drift-diffusion model, which also provides an estimation of the electron spin lifetime  $\tau_s = 15 \pm 5$  ns at the  $\Delta$ -valleys, which is in good agreement with theoretical calculations reported in Refs. 29, 52, and 54. These results lay the groundwork for spintronic devices based on bulk Si.

The authors would like to thank M. Jamet for a critical reading of the manuscript and fruitful discussions. Partial funding is acknowledged to the CARIPLO Project SEARCH-IV (Grant No. 2013-0623).

<sup>1</sup>Optical orientation (*Modern Problems in Condensed Matter Sciences*, edited by F. Meier and B. P. Zakharchenya (Elsevier, Amsterdam, 1984), Vol. 8.

<sup>2</sup>I. Zutic, J. Fabian, and S. Das Sarma, *Rev. Mod. Phys.* **76**, 323 (2004).

<sup>3</sup>G. Lampel, *Phys. Rev. Lett.* **20**, 491 (1968).

<sup>4</sup>M. S. Tyagi and R. Van Overstraeten, *Solid State Electron.* **26**, 577 (1983).

<sup>5</sup>J. A. del Alamo and R. M. Swanson, *Solid State Electron.* **30**, 1127 (1987).

<sup>6</sup>R. Parsons, *Phys. Rev. Lett.* **23**, 1152 (1969).

<sup>7</sup>D. Pierce and F. Meier, *Phys. Rev. B* **13**, 5484 (1976).

<sup>8</sup>F. Ciccacci, S. F. Alvarado, and S. Valeri, *J. Appl. Phys.* **53**, 4395 (1982).

<sup>9</sup>F. Ciccacci, H.-J. Drouhin, C. Hermann, R. Houdre, and G. Lampel, *Appl. Phys. Lett.* **54**, 632 (1989).

<sup>10</sup>R. Allenspach, F. Meier, and D. Pescia, *Phys. Rev. Lett.* **51**, 2148 (1983).

<sup>11</sup>F. Bottegoni, G. Isella, S. Cecchi, and F. Ciccacci, *Appl. Phys. Lett.* **98**, 242107 (2011).

<sup>12</sup>F. Bottegoni, A. Ferrari, G. Isella, M. Finazzi, and F. Ciccacci, *Phys. Rev. B* **85**, 245312 (2012).

<sup>13</sup>F. Pezzoli, F. Bottegoni, D. Trivedi, F. Ciccacci, A. Giorgioni, P. Li, S. Cecchi, E. Grilli, Y. Song, M. Guzzi, H. Dery, and G. Isella, *Phys. Rev. Lett.* **108**, 156603 (2012).

<sup>14</sup>A. Ferrari, F. Bottegoni, G. Isella, S. Cecchi, and F. Ciccacci, *Phys. Rev. B* **88**, 115209 (2013).

<sup>15</sup>P. Li and H. Dery, *Phys. Rev. Lett.* **105**, 037204 (2010).

<sup>16</sup>J. L. Cheng, J. Rioux, J. Fabian, and J. E. Sipe, *Phys. Rev. B* **83**, 165211 (2011).

<sup>17</sup>N. Sircar and D. Bougeard, *Phys. Rev. B* **89**, 041301 (2014).

<sup>18</sup>B. T. Jonker, G. Kioseoglou, A. T. Hanbicki, C. H. Li, and P. E. Thompson, *Nat. Phys.* **3**, 542 (2007).

<sup>19</sup>I. Appelbaum, B. Huang, and D. J. Monsma, *Nature* **447**, 295 (2007).

<sup>20</sup>B. Huang, D. J. Monsma, and I. Appelbaum, *Phys. Rev. Lett.* **99**, 177209 (2007).

<sup>21</sup>O. M. J. van't Erve, A. T. Hanbicki, M. Holub, C. H. Li, C. Awo-Affouda, P. E. Thompson, and B. T. Jonker, *Appl. Phys. Lett.* **91**, 212109 (2007).

<sup>22</sup>C. H. Li, G. Kioseoglou, O. M. J. van't Erve, P. E. Thompson, and B. T. Jonker, *Appl. Phys. Lett.* **95**, 172102 (2009).

<sup>23</sup>L. Grenet, M. Jamet, P. Noe, V. Calvo, J.-M. Hartmann, L. E. Nistor, B. Rodmacq, S. Auffret, P. Warin, and Y. Samson, *Appl. Phys. Lett.* **94**, 032502 (2009).

<sup>24</sup>A. Jain, J.-C. Rojas-Sanchez, M. Cubukcu, J. Peiro, J.-C. Le Breton, C. Vergnaud, E. Augendre, L. Vila, J.-P. Attané, S. Gambarelli, H. Jaffrès, J.-M. George, and M. Jamet, *Eur. Phys. J. B* **86**, 140 (2013).

<sup>25</sup>S. P. Dash, S. Sharma, R. S. Patel, M. P. de Jong, and R. Jansen, *Nature* **462**, 491 (2009).

- <sup>26</sup>E. Shikoh, K. Ando, K. Kubo, E. Saitoh, T. Shinjo, and M. Shiraishi, *Phys. Rev. Lett.* **110**, 127201 (2013).
- <sup>27</sup>A. Dankert, R. S. Dulal, and S. P. Dash, *Sci. Rep.* **3**, 3196 (2013).
- <sup>28</sup>T. Sasaki, Y. Ando, M. Kamenno, T. Tahara, H. Koike, T. Oikawa, T. Suzuki, and M. Shiraishi, *Phys. Rev. Appl.* **2**, 034005 (2014).
- <sup>29</sup>P. Li and H. Dery, *Phys. Rev. Lett.* **107**, 107203 (2011).
- <sup>30</sup>H. Dery, Y. Song, P. Li, and I. Zutic, *Appl. Phys. Lett.* **99**, 082502 (2011).
- <sup>31</sup>R. Jansen, *Nat. Mater.* **11**, 400 (2012).
- <sup>32</sup>J. Li, L. Qing, H. Dery, and I. Appelbaum, *Phys. Rev. Lett.* **108**, 157201 (2012).
- <sup>33</sup>O. Restrepo and W. Windl, *Phys. Rev. Lett.* **109**, 166604 (2012).
- <sup>34</sup>Y. Song, O. Chalaev, and H. Dery, *Phys. Rev. Lett.* **113**, 167201 (2014).
- <sup>35</sup>E. Saitoh, M. Ueda, H. Miyajima, and G. Tatara, *Appl. Phys. Lett.* **88**, 182509 (2006).
- <sup>36</sup>K. Ando, M. Morikawa, T. Trypiniotis, Y. Fujikawa, C. H. W. Barnes, and E. Saitoh, *Appl. Phys. Lett.* **96**, 082502 (2010).
- <sup>37</sup>F. Bottegoni, A. Ferrari, G. Isella, M. Finazzi, and F. Ciccacci, *Phys. Rev. B* **88**, 121201 (2013).
- <sup>38</sup>G. Isella, F. Bottegoni, A. Ferrari, M. Finazzi, and F. Ciccacci, *Appl. Phys. Lett.* **106**, 232402 (2015).
- <sup>39</sup>S. K. Khamari, S. Porwal, V. K. Dixit, and T. K. Sharma, *Appl. Phys. Lett.* **104**, 042102 (2014).
- <sup>40</sup>F. Bottegoni, A. Ferrari, S. Cecchi, M. Finazzi, F. Ciccacci, and G. Isella, *Appl. Phys. Lett.* **102**, 152411 (2013).
- <sup>41</sup>F. Bottegoni, M. Celebrano, M. Bollani, P. Biagioni, G. Isella, F. Ciccacci, and M. Finazzi, *Nat. Mater.* **13**, 790 (2014).
- <sup>42</sup>F. Bottegoni, A. Ferrari, F. Rortais, C. Vergnaud, A. Marty, G. Isella, M. Finazzi, M. Jamet, and F. Ciccacci, *Phys. Rev. B* **92**, 214403 (2015).
- <sup>43</sup>G. F. Koster, J. O. Dimmock, R. G. Wheeler, and H. Statz, *Lecture Notes in Computer Science*, edited by R. Klix, W. Dittmann, and R. Stenzel (Springer Verlag, Cambridge, MA, 1994).
- <sup>44</sup>R. Nouchi, *J. Appl. Phys.* **116**, 184505 (2014).
- <sup>45</sup>K. Ando and E. Saitoh, *Nat. Commun.* **3**, 629 (2012).
- <sup>46</sup>F. Bottegoni, H.-J. Drouhin, G. Fishman, and J.-E. Wegrowe, *Phys. Rev. B* **85**, 235313 (2012).
- <sup>47</sup>K. Ando, M. Morikawa, T. Trypiniotis, Y. Fujikawa, C. H. W. Barnes, and E. Saitoh, *J. Appl. Phys.* **107**, 113902 (2010).
- <sup>48</sup>A. D. Rakić, A. B. Djurišić, J. M. Elazar, and M. L. Majewski, *Appl. Opt.* **37**, 5271 (1998).
- <sup>49</sup>M. A. Green and M. J. Keevers, *Prog. Photovoltaics Res. Appl.* **3**, 189 (1995).
- <sup>50</sup>S. Birner, T. Zibold, T. Andlauer, T. Kubis, M. Sabathil, A. Trellakis, and P. Vogl, *IEEE Trans. Electron Devices* **54**, 2137 (2007).
- <sup>51</sup>*Lecture Notes in Computer Science*, edited by R. Klix, W. Dittmann, and R. Stenzel (Springer Verlag, Cambridge, MA, 1994).
- <sup>52</sup>Y. Song and H. Dery, *Phys. Rev. B* **86**, 085201 (2012).
- <sup>53</sup>A. J. Sabbah and D. M. Riffe, *Phys. Rev. B* **66**, 165217 (2002).
- <sup>54</sup>J. L. Cheng, M. W. Wu, and J. Fabian, *Phys. Rev. Lett.* **104**, 016601 (2010).
- <sup>55</sup>J. Rioux and J. E. Sipe, *Phys. Rev. B* **81**, 155215 (2010).
- <sup>56</sup>C. Guite and V. Venkataraman, *Appl. Phys. Lett.* **101**, 252404 (2012).
- <sup>57</sup>P. Li, Y. Song, and H. Dery, *Phys. Rev. B* **86**, 085202 (2012).
- <sup>58</sup>F. Rortais, S. Oyarzún, F. Bottegoni, J.-C. Rojas-Sánchez, P. Laczkowski, A. Ferrari, C. Vergnaud, C. Ducruet, C. Beigné, N. Reyren, A. Marty, J.-P. Attané, L. Vila, S. Gambarelli, J. Widiez, F. Ciccacci, H. Jaffrès, J.-M. George, and M. Jamet, *J. Phys. Condens. Matter* **28**, 165801 (2016).